LARGE EDDY SIMULATION OF NATURAL CONVECTION BOUNDARY LAYER ON A VERTICAL CYLINDER

D. G. Barhaghi [a] and L. Davidson [a] and R. Karlsson [a,b]

[a]Division of Thermo and Fluid Dynamics, Department of Mechanical Engineering,
Chalmers University of Technology, SE-412 96 Göteborg, Sweden
[b]Vattenfall Utveckling AB, SE-814 26 Älvkarleby, Sweden

ABSTRACT

Large eddy simulation of natural convection boundary layer along a constant temperature vertical cylinder is studied and the results are compared with the existing experimental data. The highest local Grashof number is $Gr_z = 5 \times 10^{11}$. It is shown that although there are some discrepancies between the results in the region close to the wall, there is qualitative agreement between them. In order to verify the credibility of the simulations, cross correlation of Reynolds stresses is studied and interpreted.

KEYWORDS

Large eddy simulation, LES, Natural convection, Free convection, Cylindrical coordinate system, Shell and tube, Boundary layer

INTRODUCTION

Natural convection is an interesting scientific subject for which many aspects need further research. The applications include not only industrial fields like power generators, reactors, turbines, heat exchangers and other power conversion devices, but also natural phenomena like atmospheric and oceanic currents, bio-heat transfer, green house effects and heat transfer in stellar atmospheres.

Compared to the number of experimental and numerical researches which have been carried out for other methods of heat transfer, few belong to the natural convection field. Among the experimental researches, the latest is that reported by Tsuji and Nagano (1988b). In that work, characteristics of natural convection boundary layer are compared with the previous investigations. It is shown

that natural convection boundary layer has a unique turbulent structure which is rarely seen in other turbulent boundary layers. The results suggest that for values of y^+ between 20 to 100, $\overline{u'v'}$ is not correlated with the mean velocity gradient, $\partial\overline{u}/\partial y$. However, comparison of Reynolds shear stress with previous experiments showed a different behavior near the wall. Although no negative region was observed by Tsuji and Nagano (1988b), almost all previous works had shown a negative region close to the wall. It is also shown that the cross-correlation coefficient for shear stress ($R_{\overline{u'v'}} = \overline{u'v'}/\sqrt{\overline{u'^2} \times \overline{v'^2}}$) becomes zero near the wall which is in contradiction to analytical analysis.

Turbulent natural convection around a heated vertical slender cylinder was studied by Persson and Karlsson (1996) and new turbulent structures were presented for the near wall region. Again it was shown that there exists a negative shear stress region close to the wall. Comparing normal stresses and temperature fluctuations with those proposed by Tsuji and Nagano (1988b), different behavior can be observed between these two experiments. Although the temperature fluctuations presented by Tsuji and Nagano (1988b) are larger than the stream-wise normal stress, it is vice versa in Persson and Karlsson (1996) work. However the location of the peaks remains in close agreement.

Natural convecting boundary layers have also been studied using DNS or LES. However, most of the studies include flows either in cavities or differentially heated channels. Among them are researches conducted by Miki et al. (1993), Versteegh and Nieuwstadt (1998), and Peng and Davidson (2001).

From previous investigations it could be found that natural convection phenomenon has still many aspects which are not clear and there are some other aspects for which there is no consensus. Another fact is that very few researches have been conducted on the natural convective boundary layer along a vertical cylinder and most of the studies are performed on flat plates, channels or horizontal cylinders. This fact besides existence of an experimental apparatus in the Mechanical Engineering Department of Chalmers University of Technology, created the motivation for designing an LES problem in order to study the natural convection heat transfer along a vertical cylinder.

GEOMETRY AND GRID SETUP

As it is shown in Figure 1, a sector of a cylindrical concentric vertical shell and tube is adopted as computational domain. All the dimensions are in millimeters. The motivation for using such a geometry was an experimental equipment with almost the same dimensions at the Department. The reason for choosing such a geometrical configuration is that although an idealized natural convecting boundary layer takes place in infinite surroundings, it is nearly impossible to achieve such an ideal condition neither in experiments nor in numerical calculations. Both experiments and calculations are very sensitive to the location of the infinite boundaries and any disturbances there. An inlet and outlet are designed to prevent stratification in the stagnant region which would affect the boundary layer growth near the hot tube.

The angular extent of the geometry was chosen by comparing the results of different geometries. An ideal angle should cover all turbulent structures and give averaged two-dimensional angle-independent results. In this work, different angles, $\theta = 18^o$, 36^o, 54^o, 72^o and 90^o have been applied to the numerical domain.

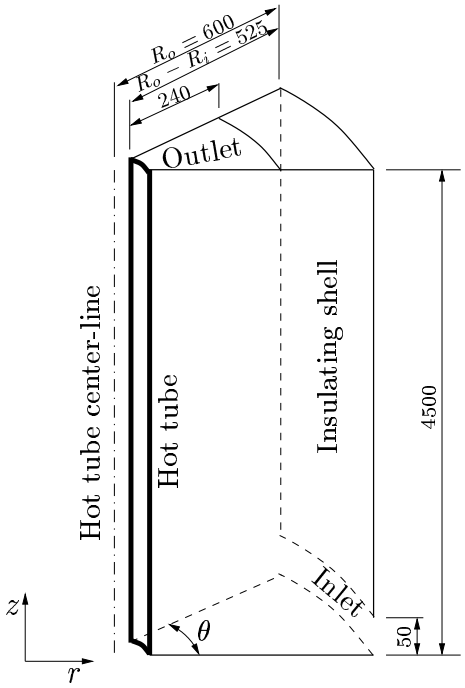

Figure 1: Computational geometry

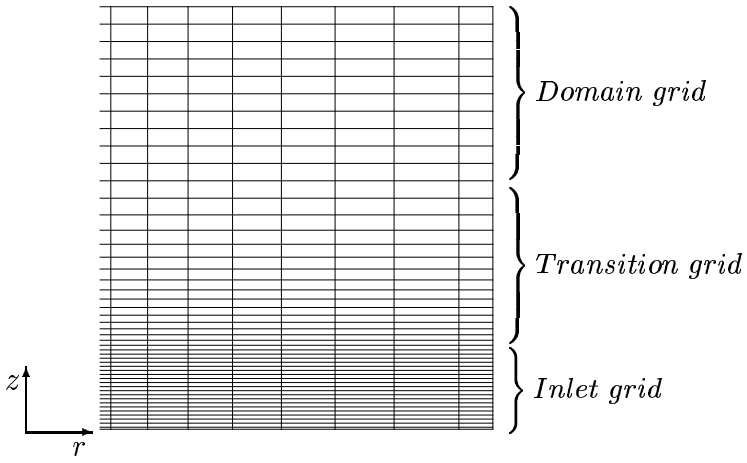

Figure 2: Grid configuration

Having studied the flow by different grid sizes, a final $98 \times 402 \times 162$ grid (r, z and θ directions) with $\theta = 90^o$ was chosen.

Different grid densities were applied at the inlet in the z-direction compared to the rest of the domain. The reason was that at the inlet the flow is in the radial direction and a turbulent three dimensional flow is introduced at the inlet. Therefore, in order to resolve these small structures a finer mesh was applied. A stretching of 9 percent is used in the transition between the inlet region and the main part of the domain, see Figure 2.

The spatial resolution along the hot cylinder is $\Delta\theta^+ < 3.5$ in the span-wise direction and $\Delta z^+ < 55$ in the stream-wise direction. The highest value for perpendicular non-dimensional distance for the wall adjacent node is $(r - R_i)^+ = 0.32$. It is found that the maximum SGS viscosity (ν_t) in the boundary layer is less than 50% of fluid viscosity and in the region $(r - R_i)^+ < 100$ it is less than 10% of fluid viscosity indicating that the boundary layer is very well resolved (see Barhaghi (2004)).

NUMERICAL METHOD

Governing Equations

The continuity, Navier-Stokes and energy equations in cylindrical coordinate system are solved. The Smagorinsky model is chosen in order to model sub-grid scales. In the momentum equations, the turbulent diffusive cross terms arising from $\frac{\partial}{\partial x_j}\left(\nu_{eff}\frac{\partial \overline{v_j}}{\partial x_i}\right)$ are neglected.

Finite Volume Approach

A conventional finite volume method (Versteegh and Malalasekera, 1995) is used to solve the governing equations. As it is very important not to dissipate the turbulence by conventional numerical schemes, it is customary to discretize the governing equations by central difference scheme. However, this approach causes a so called unphysical fluctuation or wiggle problem which

is related to the unboundedness of the central difference scheme. Especially, this problem can be encountered in regions where turbulence intensity is not high enough or in laminar regions and in regions where the grid is not fine enough. Both of these problems occur in the present LES simulations near the inlet. Using pure central difference scheme, these unphysical fluctuations were generated near the inlet and propagated throughout the computational domain. To remedy this problem, a blend of central difference scheme with deferred correction (Ferziger and Peric, 1996) and Van-Leer scheme were used (Dahlström and Davidson, 2003).

The second-order Crank-Nicolson scheme is used in order to discretize the equations in time. The numerical procedure is based on an implicit, fractional step technique with a multi-grid pressure Poisson solver (Emvin, 1997) and a non-staggered grid arrangement (Davidson and Peng, 2003).

Boundary Conditions and Fluid Data

Simulation of laminar regions with LES method may provoke the problem of unphysical fluctuations. In order to create turbulence at the inlet, the velocity field of the DNS of a channel flow for which the bulk velocity was $0.6m/s$, is scaled and implemented as inlet boundary condition for velocities. No slip boundary condition is used for all solid boundaries.

For the temperature, Dirichlet boundary condition is applied at the hot tube and the inlet. The temperature is set to 80^oC and 25^oC on the hot tube and at the inlet respectively. Except for the outlet, homogeneous Neumann boundary condition is used over all remaining boundaries.

At the outlet, for both temperature and velocities, a convective boundary condition (Sohankar et al., 1998) is applied.

The dynamic viscosity and the Prandtl number of the fluid are $\mu = 18.9 \times 10^{-6}$ and $Pr = 0.7$, respectively.

In order to accelerate the convergence of the numerical computations to a fully developed condition, either the results of a 2D-RANS simulation or whenever existed, the results of previous simulations for different grid configuration, were interpolated and applied as initial boundary condition.

RESULTS

Once fully developed condition is achieved, sampling can be started. Sampling should last sufficiently long to ensure independent results regarding the number of samples. This is checked by comparing the results of two different averaged result with different number of samples.

Fully Developed Flow Assessment

In order to assess whether or not the flow has reached to the state of fully developed condition so that sampling can be started, the instantaneous local Nusselt number at different heights has been calculated. The instantaneous, filtered and averaged Nusselt number are shown in Figure 3 for two vertical levels, one near the inlet and one near the outlet. It can be observed that almost for the last 15000 time steps, Nusselt number fluctuates uniformly. The filtered value, which is an average of 2000 instantaneous neighboring Nusselt numbers, shows it more clearly. These figures verify that the flow has reached the state of fully developed condition and statistical averaging can be started.

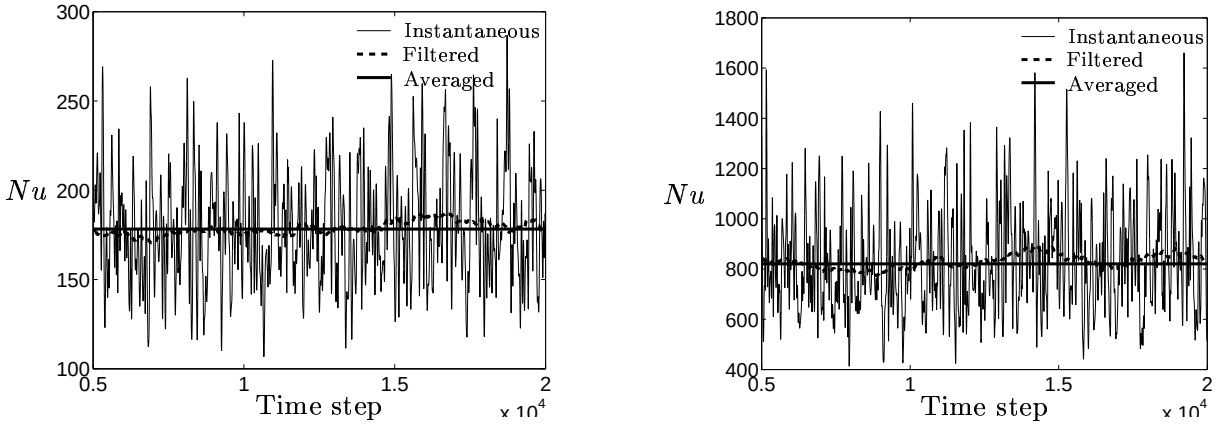

(a) Nusselt no. at $z/H = 0.2$

(b) Nusselt no. at $z/H = 0.9$

Figure 3: Assessment of fully developed flow regarding local Nusselt number

Figure 4 shows velocity and Reynolds shear stress obtained from the three last 5000 time steps of simulation. As can be seen, very little difference exists between the results. For the shear stress, the big difference lies in the outer region near the outer shell far away from the boundary layer. Again from these two figures, it can be seen that the simulation has reached to the state of fully developed condition. Hereafter, the statistics and averaged values are calculated using the last 15000 time steps.

Grid Independent Result

In numerical simulations, grid independent result is always desirable. This can be checked by comparing the results of different grids. However, as LES is inherently dependent on the grid resolution, no final grid-independent result exists. In this computations, a final 98×402 mesh in r and z directions, respectively, is chosen. However it is found that the angular width of the domain has a crucial effect on the final results. This is shown in Figure 5 where velocity and shear stress for different sizes of the computational domain are depicted. Although the grid spacing in the θ-direction is the same for all grids it can be seen that the difference between the curves for

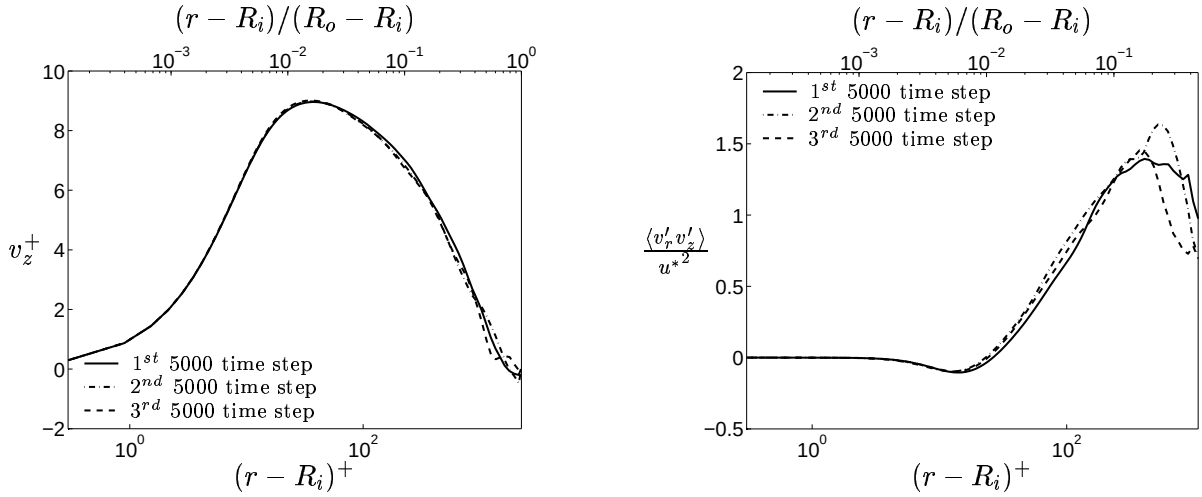

(a) Dimensionless velocity

(b) Reynolds shear stress

Figure 4: Velocity and shear stress at $z/H = 0.8, Gr = 2.9 \times 10^{11}$ for contiguous averaged data

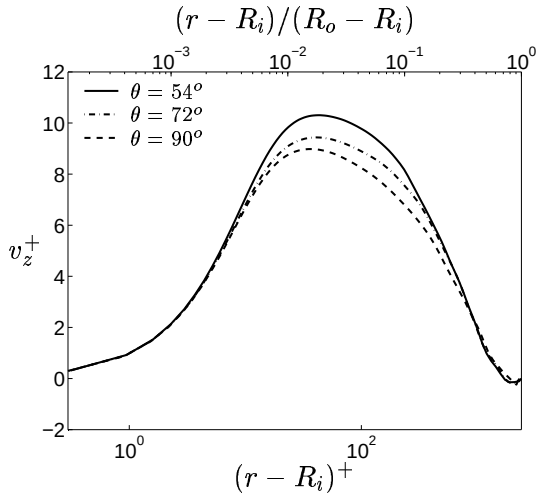

(a) Dimensionless velocity

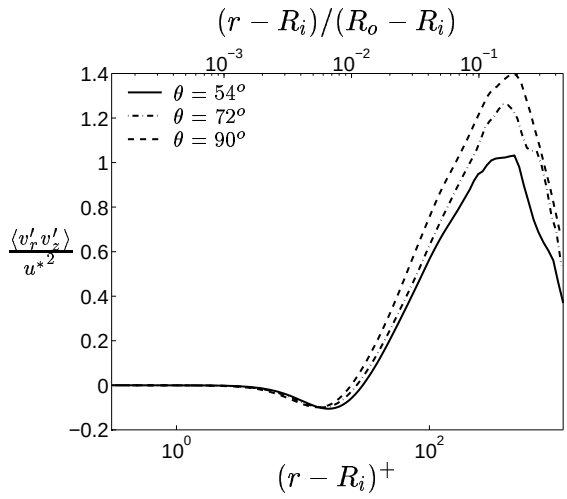

(b) Reynolds shear stress

Figure 5: Velocity and shear stress at $z/H = 0.8, Gr_z = 2.9 \times 10^{11}$ for different domains

$\theta = 72^o$ and $\theta = 90^o$ is less than that for $\theta = 54^o$ and $\theta = 72^o$, for both velocity and shear stress. Although it is not shown, the difference between the results of other grids with $\theta = 18^o$, $\theta = 36^o$ was even larger. However, as can be seen in Figure 6, the difference between Nusselt numbers for grids with $\theta = 72^o$ and $\theta = 90^o$ is negligible compared to that between $\theta = 54^o$ and $\theta = 72^o$.

Mean Fluid Flow and Heat Transfer Parameters

Figures 7(a) and 7(b) compare the results of the present study and previous experiments. As can be seen, although the results of present study are in good agreement with the results of Tsuji and Nagano (1988a), the results of Persson and Karlsson (1996) are rather different.

As a common behavior in all graphs, however, except for a very small distance from the wall , $(r - R_i)^+ < 1.2$, velocity does not follow the law of the wall, $v_z^+ = (r - R_i)^+$, the same way it does for forced convecting boundary layers.

However, Figure 7(b) shows that temperature follows the law of the wall in the region $(r - R_i)^+ < 5$, alike forced convecting flows.

Although no self similar behavior regarding dimensionless velocity v_z^+ could be observed from the

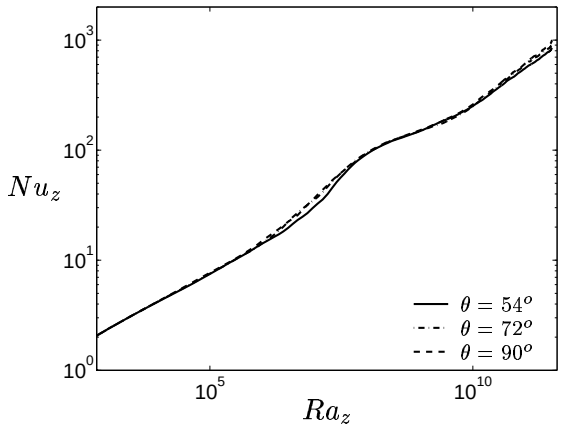

Figure 6: Nusselt number at $z/H = 0.9, Gr_z = 4.2 \times 10^{11}$ for different domains

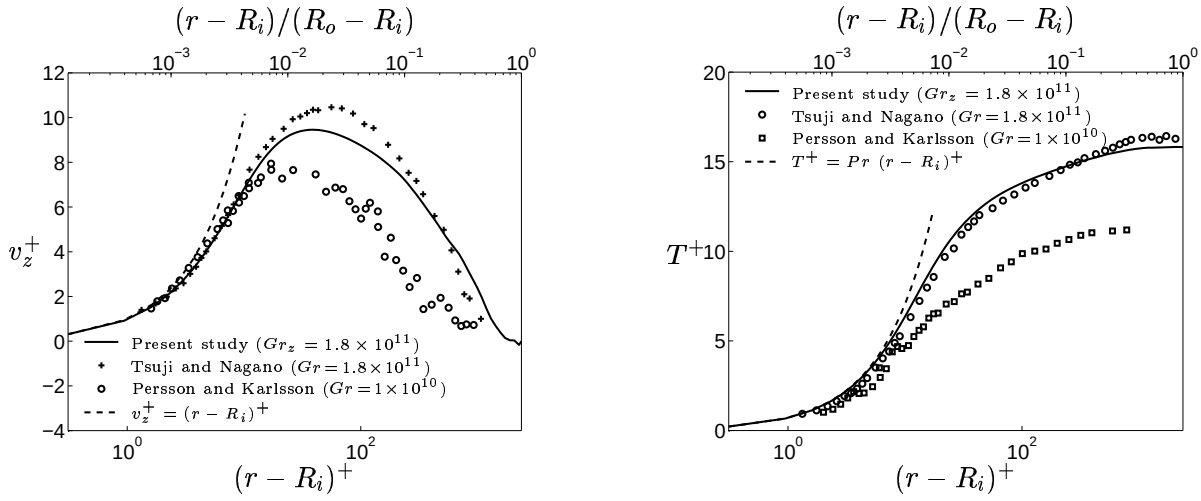

(a) Dimensionless velocity

(b) Dimensionless temperature

Figure 7: Comparison of velocity and temperature with experimental data

results of Tsuji and Nagano (1988a), graphs of the v_z^+ vs. $(r-R_i)^+$ in this study collapse on each other, showing a self similar behavior, see Figure 8.

Finally, Figure 9 shows variation of Nusselt number as a function of Rayleigh number. Compared to the results of Tsuji and Nagano (1988a) and proposed correlation for the laminar region, there is a very good agreement for both the laminar and the turbulent region. However, the major difference is in the transition region. The transition for the studied flow seems to be starting from $Ra_z = 10^6$ compared to the flow along the flat plate for which transition starts from $Ra = 8\times10^8$. The difference is probably due to first the turbulent inlet, second, inherent difference between characteristics of boundary layer along a vertical flat plat and a vertical slender cylinder and third, existence of the outer shell which embraces the whole cylinder and provokes instabilities by creating some recirculating flows in the proximity of boundary layer.

Another difference in Figure 9 is the overshoot of Nusselt number in the commencement of turbulent boundary layer which was not observed by Tsuji and Nagano (1988a) but had been mentioned in previous researches (e.g. Cheesewright, 1968).

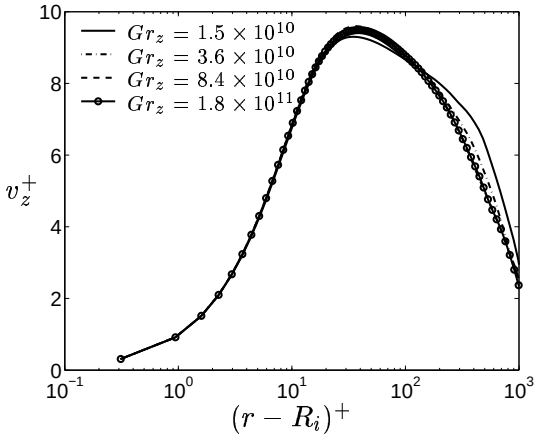

Figure 8: Dimensionless velocity profiles for different Grashof numbers

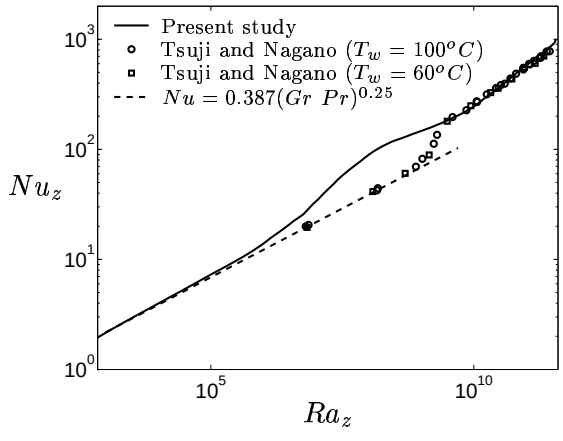

Figure 9: Nusselt number as a function of Rayleigh number

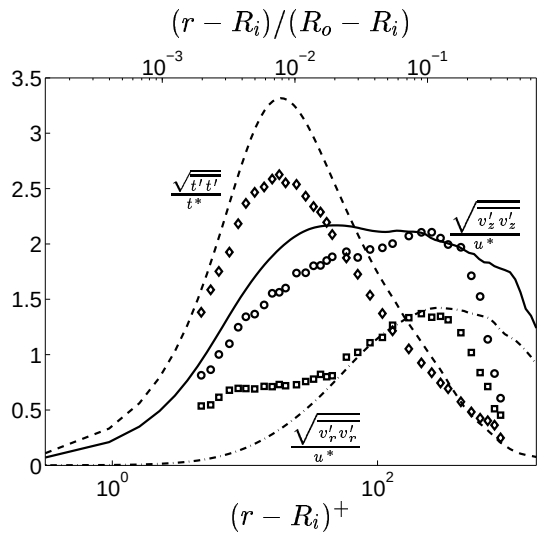

(a) Experimental data from Tsuji and Nagano (1988a), $Gr = 8.99 \times 10^{10}$

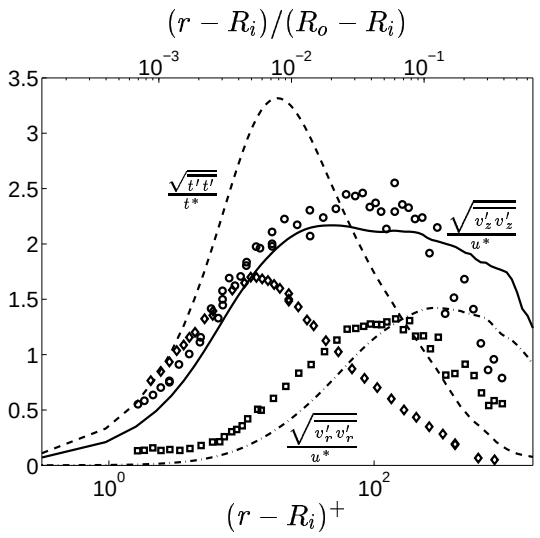

(b) Experimental data from Persson and Karlsson (1996), $Gr = 1 \times 10^{10}$

Figure 10: Normal stresses and temperature fluctuations. Lines: simulation; markers: experiments

Reynolds Stresses and Turbulent Heat Fluxes

Figure 10 compares normal stresses and temperature fluctuations with the experimental data. In Figure 10(a), both the predicted $\sqrt{\overline{t't'}}/t^*$ and the stream-wise normal stress have higher values compared to the experimental data for the flat plate. wall-normal stress, however, have smaller values for $(r - R_i)^+ < 92.5$. No constant value region such as that observed in the experiment for $\sqrt{\overline{v'^2}}/u^*$ in the $7.5 < (r - R_i)^+ < 40$ can be observed in the LES-simulations. Nevertheless, the graphs are qualitatively in a good agreement and locations of maxima match each other.

Discrepancies between experiments and computations are even larger in Figure 10(b). Contrary to computations and the other experimental data, normalized temperature fluctuations are smaller than stream-wise velocity fluctuations. Also, locations of maxima are under predicted.

Experimental wall-normal stress in Figure 10(b), shows the same behavior as computations contrary to that presented by Tsuji and Nagano (1988a). However, none of the experiments show a tendency for this parameter to become zero sufficiently close to the wall, reflecting the unreliability of measurements close to the wall.

Reynolds shear stress together with stream-wise and wall-normal turbulent heat fluxes are shown in Figure 11. Again, although the values in Figure 11(a) are in close agreement, this is not the case in Figure 11(b). While wall normal turbulent heat flux remains positive close to the wall for both computations and experiments in Figure 11(a), it gets negative values for experiment shown in Figure 11(b). Also contrary to the computation and experiment shown in Figure 11(b), no negative shear stress can be observed in the experimental values shown in Figure 11(a). However, this negative region shown in Figure 11(b) is shifted toward the wall for experiment.

In the experiment of Persson and Karlsson (1996) no negative region close to the wall for stream-wise turbulent heat flux can be observed, albeit the existence of this region is confirmed by Tsuji and Nagano (1988b).

Finally, Figure 12 compares the cross correlation coefficient between the shear stress and the

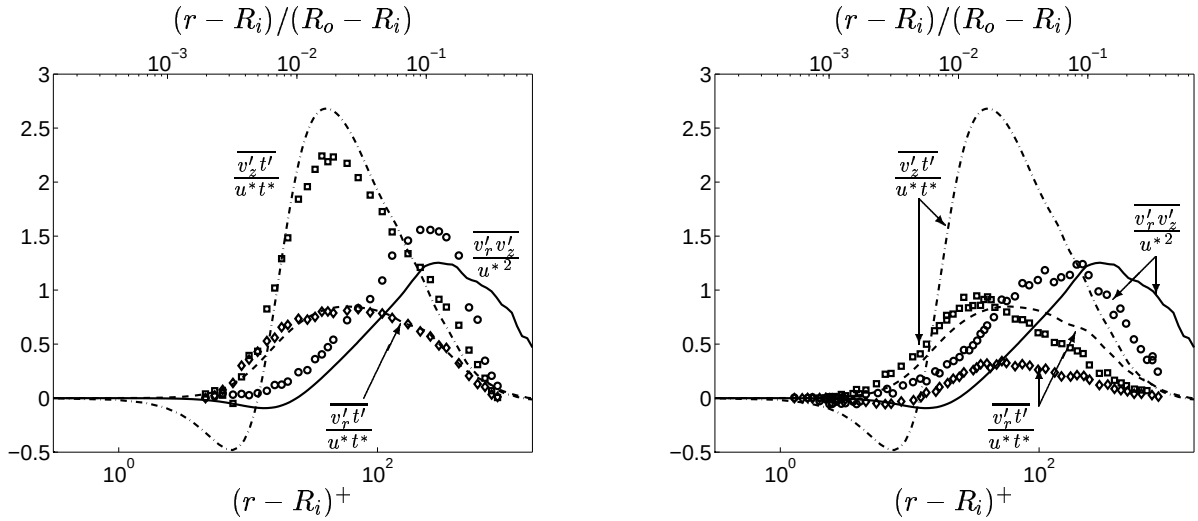

(a) Experimental data from Tsuji and Nagano (1988a), $Gr = 8.99 \times 10^{10}$

(b) Experimental data from Persson and Karlsson (1996), $Gr = 2 \times 10^{10}$

Figure 11: Turbulent shear stress and heat fluxes. Lines: simulation; markers: experiments

normal stresses. From the Taylor expansion, $\overline{v_r' v_z'} = \mathcal{O}(r^3)$, $\overline{v_r'^2} = \mathcal{O}(r^4)$ and $\overline{v_z'^2} = \mathcal{O}(r^2)$. So R_{uv} should have a constant value very close to the wall when r approaches zero. This can be found from Figure 12 for the present simulation and Persson and Karlsson (1996), for which the constant values are $R_{uv} \approx -0.3$ and $R_{uv} \approx -0.09$, respectively. As this coefficient becomes zero in the experiment of Tsuji and Nagano (1988a), again it can be deduced that the measured stresses for this experiment are unreliable in the region close to the wall.

CONCLUSIONS

Natural convection boundary layer along a constant temperature vertical cylinder is studied. It is shown that linear law of the wall for the velocity is valid just for a very small region close to the wall, $(r - R_i)^+ < 1.2$. The profiles of the velocity collapse on each other in the turbulent region showing a self similar behavior.

Nusselt number is compared with the experimental values and it is deduced that the transition

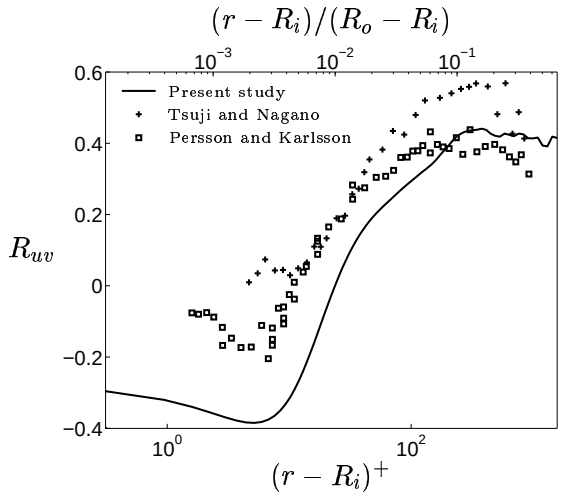

Figure 12: Cross correlation coefficient comparison, $R_{uv} = \frac{\overline{v_r' v_z'}}{\sqrt{\overline{v_r'^2} \times \overline{v_z'^2}}}$

for this simulation has started earlier compared to experiments on the vertical wall. The existence of an overshoot in the commencement of turbulent region is also verified.

Comparison of the calculated Reynolds stresses with those obtained from experiments shows that the measured values are not reliable close to the wall. This is also verified by considering cross correlation coefficient.

Existence of a region with negative values for both shear stress and stream-wise turbulent heat flux is shown and it is verified that the wall normal heat flux remains positive even close to the wall.

ACKNOWLEDGMENTS

Financial support from the Swedish Research Council and part of the computer resources provided by the Center for Parallel Computing (PDC), KTH are greatly acknowledged. Authors are also indebted to Dr. Shia-Hui Peng for his support and sharing his ideas and knowledge.

REFERENCES

Barhaghi, D. G., 2004. Dns and les of turbulent natural convection boundary layer. Thesis for Licentiate of Engineering 04/05, Dept. of Thermo and Fluid Dynamics, Chalmers University of Technology, Göteborg, Sweden.

Cheesewright, R., 1968. Turbulent natural convection from a plane vertical surface. Journal of Heat Transfer 90, 1–8.

Dahlström, S., Davidson, L., 2003. Large eddy simulation applied to a high-reynolds flow around an airfoil close to stall. AIAA paper 2003-0776.

Davidson, L., Peng, S.-H., 2003. Hybrid LES-RANS: A one-equation SGS model combined with a $k - \omega$ model for predicting recirculating flows. International Journal for Numerical Methods in Fluids 43, 1003–1018.

Emvin, P., 1997. The full multigrid method applied to turbulent flow in ventilated enclosures using structured and unstructured grids. Ph.D. thesis, Dept. of Thermo and Fluid Dynamics, Chalmers University of Technology, Göteborg.

Ferziger, J. H., Peric, M., 1996. Computational Methods for Fluid Dynamics. Springer-Verlag, Berlin.

Miki, Y., Fukuda, K., Taniguchi, N., 1993. Large eddy simulation of turbulent natural convection in concentric horizontal annuli. Int. J. Heat and Fluid Flow 14, 210–216.

Peng, S.-H., Davidson, L., 2001. Large eddy simulation for turbulent buoyant flow in a confined cavity. International Journal of Heat and Fluid Flow 22, 323–331.

Persson, N. J., Karlsson, R. I., 1996. Turbulent natural convection around a heated vertical slender cylinder. In: 8th Int. Symp. on Applications of Laser Techniques to Fluid Mechanics. Lisbon.

Sohankar, A., Norberg, C., Davidson, L., 1998. Low-Reynolds number flow around a square cylinder at incidence: Study of blockage, onset of vortex shedding and outlet boundary condition. International Journal for Numerical Methods in Fluids 26, 39–56.

Tsuji, T., Nagano, Y., 1988a. Characteristics of a turbulent natural convection boundary layer along a vertical flat plate. International Journal of Heat and Mass Transfer 31 (8), 1723–1734.

Tsuji, T., Nagano, Y., 1988b. Turbulence measurements in a natural convection boundary layer along a vertical flat plate. International Journal of Heat and Mass Transfer 31 (10), 2101–2111.

Versteegh, H. K., Malalasekera, W., 1995. An Introduction to Computational Fluid Dynamics - The Finite Volume Method. Longman Scientific & Technical, Harlow, England.

Versteegh, T. A. M., Nieuwstadt, F. T. M., 1998. Turbulent budgets of natural convection in an infinite, differentially heated, vertical channel. International Journal of Heat and Fluid Flow 19, 135–149.